Heat Mass Transfer (2005) 41: 367–374
DOI 10.1007/s00231-004-0551-3

ORIGINAL

Md. Anwar Hossain · D. A. S Rees

Natural convection flow of water near its density maximum in a rectangular enclosure having isothermal walls with heat generation

Received: 15 July 2003 / Published online: 10 September 2004

Abstract We consider unsteady laminar natural convection flow of water subject to density inversion in a rectangular cavity formed by isothermal vertical walls with internal heat generation. The top and bottom horizontal walls are considered to be adiabatic, whereas the temperature of the left vertical wall is assumed to be greater than that of the right vertical wall. The equations are non-dimensionalized and are solved numerically by an upwind finite difference method together with a successive over-relaxation (SOR) technique. The effects of both heat generation and variations in the aspect ratio on the streamlines, isotherms and the rate of heat transfer from the walls of the enclosure are presented. Investigations are performed for water taking Prandtl number to be $\mathrm{Pr} = 11.58$ and the Rayleigh number to be $\mathrm{Ra} = 10^5$.

List of symbols

C_p	specific heat at constant pressure, J/kg K
g	gravitational acceleration, m/s^2
Ra	Rayleigh number
H	enclosure height, m
k	effective thermal conductivity of the media, W/m K
p	fluid pressure, Pa
Pr	Prandtl number
t	time, s
T	temperature, °C
u	velocity in x-direction, m/s
U_0	(ν/H) reference velocity, m/s
v	velocity in y-direction, m/s
x, y	Cartesian coordinates, m
X, Y	dimensionless coordinates
β	coefficient of thermal expansion of fluid, 1/K
θ	dimensionless temperature
λ	dimensionless heat absorption/generation parameter
μ	effective dynamic viscosity, Pa/s
ν	effective kinematic viscosity, μ/ρ
ρ	fluid density at reference temperature, T_c
τ	dimensionless time
ψ	streamfunction, m^2/s
Ω	dimensionless vorticity

M. A. Hossain (✉)
Department of Mathematics, University of Dhaka,
Dhaka, 1000, Bangladesh
E-mail: anwar@udhaka.net

D. A. S Rees
Department of Mechanical Engineering,
University of Bath, Bath, BA2 7AY, UK
E-mail: D.A.S.Rees@bath.ac.uk

1 Introduction

A theoretical study of transient natural convection flow in a square cavity at high Rayleigh number was performed by Han [1]. In this analysis the heat transfer rate was calculated and found to decay in an oscillatory manner towards the steady state. Further experimental studies were carried out by Ivey [2]. Nicolette et al. [3] and Hall et al. [4] conducted numerical and experimental investigations for transient cooling in an isothermal square enclosure with one vertical wall cooled and the other three walls insulated. Good agreement was found between experimental data and numerical prediction. In studies of transient flow in an enclosure, interest is commonly directed toward the following: (a) the evolution of convective flow pattern and temperature field with time, (b) the time scale required to achieve steady-state condition, (c) determining whether there is an oscillatory or a monotonic approach to the steady-state, (d) the thickness of the boundary layer at the vertical wall when the flow approaches the steady state and (e) the characteristic velocity within the boundary layer.

It is well known that for some fluids, such as water, liquid helium and pseudobinary electronic alloy HgCdTe, the fluid density is not a monotonic function of the temperature; rather the density reaches a

maximum value at a specific temperature and decreases when deviating from that temperature. As a result, the Boussinesq approximation, which is based on the linear behaviour of density-temperature relation, is strictly not applicable to these fluids. This property, known as density inversion, can significantly change the flow field and heat transport in an enclosure. Natural convection in such a liquid is of practical importance in areas such as atmospheric and oceanic movement, ice formation and melting, and crystal growth, etc. Although the density inversion effect on natural convection has been studied extensively in the past [5–9], the great majority of these studies consider steady-state flows in closed enclosures.

Transient natural convection in water subject to density inversion was considered by Forbes and Cooper [10]. In that study, water, confined laterally and underneath by rigid insulating walls, was initially set to a uniform temperature and then the temperature of the upper surface was suddenly changed. The effect of a maximum density on transient natural convection in an enclosed rectangular cavity was also investigated by Vasseur and Robillard [11] and by Robillard and Vasseur [12, 13]. They found that the convective heat transfer, the flow pattern and the temperature profile can be influenced greatly by the presence of a density maximum of the convective fluid. Recently, Oostuizen and Paul [14] performed numerical investigations for a similar problem. On the other hand, Tong and Koster [15] investigated numerically the transient natural convection in a water layer subjected to density inversion by employing the finite element method for Rayleigh numbers up to 10^6 for a wide range of aspect ratios from 0.25 to 10.

Watson [5] analysed the effect of density inversion on the fluid flow and heat transfer in a square vessel for values of Ra, the Rayleigh number, which were less than 2×10^4. The results showed that the maximum density effect is greatest when $\Delta T = 8$°C. Seki et al. [7] investigated natural convection both numerically and experimentally in rectangular vessels. The cold vertical wall was maintained at 0°C while the hot wall temperature varied from 1 to 12°C. Lin and Nansteel [6] investigated numerically the natural convection in a square enclosure containing water near its density maximum and found multi-cellular flow structures for certain ranges of values of the density distribution parameter, which is independent of Ra.

It should be mentioned that there are several models which describe the density/temperature behaviour of water around the maximum density region. A parabolic density relationship is given by Debler [16]:

$$\rho = \rho_0\left[1 - \gamma(T - T_0)^2\right], \tag{1}$$

where $\gamma = 8.000216\times10^{-6}$ $(°C)^{-2}$, ρ_0 is the maximum density at $T_0 = 3.98$°C (for water). Later, by adding a cubic term in Eq. 10 this model was expanded to cover the temperature range from 0 to 30°C (Sun et al. [17]):

$$\rho = \rho_0\left[1 - \gamma_1(T - T_0)^2 + \gamma_2(T - T_0)^3\right]. \tag{2}$$

Additionally, Gebhart and Mollendorf [18] proposed the following density equation:

$$\rho(T, s, p) = \rho_0(s, p)\left[1 - a(s, p)|T - T_0(s, p)|^{q(s,p)}\right]. \tag{3}$$

The density variation is fitted in temperature, salinity and pressure ranges up to 20°C, 40% and 1,000 bars absolute, respectively. For pure water under 1 atmosphere at $a(0,1) = 9.297173\times10^{-6}$(°C), $T_m(0,1) = 4.029325$ °C and $q(0,1) = 1.894816$. It is to be noted that the value of $T_m(0,1)$ obtained by the regression not exactly either 3.98 nor 4°C. Though Eq. 1 is claimed to be more accurate for the temperature range up to 8°C [16], the difference in the calculated values from Eqs. 1 and 3 for the present interested temperature range (0–12°C) is found to be negligibly small ($< 0.005\%$). Hence the present work extends the previous studies of natural convection in water with density maximum inversion, by considering the density function as given by Eq. 1, confined in a rectangular cavity by bringing into account the effect of temperature dependant volumetric heat generation, q''' (W/m^3), in the flow region, that is given by Vajravelu and Hadjinicolaou [19] as below,

$$q''' = Q_0(T - T_0), \quad T \geqslant T_0, \tag{4}$$

where Q_0 is the heat generation constant. On taking into consideration this form of heat-generation Hossain and Wilson [20] have investigated recently the natural convection flow of a fluid of $Pr = 0.7$ in a fluid-saturated porous medium enclosed by non-isothermal walls.

The reduced dimensionless equations governing the flow have been simulated numerically by employing an upwind finite-difference method, together with the successive over-relaxation (SOR) iteration technique. The results are displayed graphically in terms of streamlines and isotherms, which show the combined effect of internal heat generation and density inversion for cavities with differential heating of the sidewalls. Attention is also focused on how the sidewall heat-flux varies.

2 Formulation of the problem

Consider a rectangular enclosure of height H filled with water whose temperature range is in the vicinity of the temperature corresponding to its maximum density, as shown in Fig. 1. The right and left walls are maintained at the respective constant hot and cold temperatures T_H and T_C, while the two horizontal walls are insulated. In the flow field we also allow for the effect of temperature-dependent heat generation. The volumetric rate of heat generation, q''', is given in Eq. 4 where $q''' = 0$ when $T < T_0$. We further assume that we are dealing with a laminar flow of a viscous incompressible fluid having constant properties. Free convection is considered by assuming that all thermophysical properties are constant

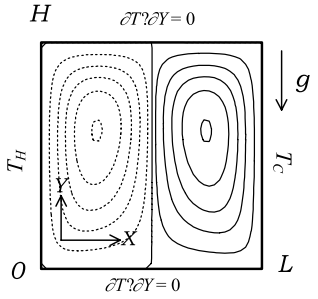

Fig. 1 The flow configuration and the coordinate system

except for the buoyancy term, which is modelled using Eq. 1. Finally, the direction of the gravitational force is as indicated in Fig. 1. In this figure dotted curves represent the regular convection flow moving in the clockwise direction and the solid curves represent convection flow moving in the anticlockwise direction; this convention is used throughout the paper.

The governing non-dimensional equations, which express the conservation of mass, momentum, energy are

$$\nabla . V = 0, \tag{5}$$

$$\frac{Du}{Dt} = -\frac{1}{\rho}\nabla p' + \nu\nabla^2 u, \tag{6}$$

$$\frac{Dv}{Dt} = -\frac{1}{\rho}\nabla p' + \nu\nabla^2 v + \rho g, \tag{7}$$

$$\frac{DT}{Dt} = \alpha\nabla^2 T + \frac{Q_0}{\rho C_p}(T - T_0), \tag{8}$$

where, τ is the time variable, u and v are the respective velocity components along the x- and y- directions, T is the temperature function, p' is the pressure, α is the thermal diffusivity, C_p is the specific heat at constant pressure and ν is the kinematic viscosity of the fluid.

Defining the modified pressure, $p' = p + \rho_0\, gy$, yields

$$\frac{\partial p'}{\partial y} = \frac{\partial p}{\partial y} - g\rho_0. \tag{9}$$

Initially, the fluid is assumed to be motionless and at uniform temperature T_0. The corresponding boundary initial and conditions are

$$u = v = 0, \quad T = T_0,$$

at $\tau = 0$ and, for $\tau > 0$,

$$u = v = 0 \quad \text{on the boundary}$$

$$T(0, y) = T_C, \quad T(L, y) = T_H, \quad \frac{\partial T(x,0)}{\partial y} = \frac{\partial T(x,H)}{\partial y} = 0. \tag{10}$$

Out of many correlations, as mentioned in the introduction, which have been used to represent the density of cold water as a function of temperature, we consider the parabolic density-temperature relationship given by Eq. 1 which had been very widely used. Introducing Eqs. 1 and 9 into 5 and 6 one gets

$$\frac{Du}{Dt} = -\frac{1}{\rho_0}\nabla p + \nu\nabla^2 u, \tag{11}$$

$$\frac{Dv}{Dt} = -\frac{1}{\rho_0}\nabla p + \nu\nabla^2 v + g\gamma(T - T_0)^2. \tag{12}$$

Now the pressure is eliminated by cross-differentiation between Eqs. 9 and 10. On defining the non-dimensional variables as:

$$\begin{aligned} X &= \tfrac{x}{L_R}, \quad Y = \tfrac{y}{L_R}, \quad t = \tfrac{\nu\tau}{L_R^2} \\ U &= \tfrac{L_R u}{\nu}, \quad V = \tfrac{L_R v}{\nu}, \quad \theta = \tfrac{T - T_0}{\Delta T}, \end{aligned} \tag{13}$$

where L_R is the reference length, $\Delta T = T_H - T_C$, the governing equations in their dimensionless form become

$$\frac{D\Omega}{Dt} = \nabla^2\Omega + 2\frac{\mathrm{Ra}}{\mathrm{Pr}}\theta\frac{\partial\theta}{\partial X}, \tag{14}$$

where

$$\Omega = -\nabla^2\psi \tag{15}$$

is the dimensionless vorticity and ψ is the dimensionless streamfunction which is defined by:

$$U = \frac{\partial\psi}{\partial Y}, \quad V = -\frac{\partial\psi}{\partial X}. \tag{16}$$

The energy equation may now be written in the form,

$$\frac{D\theta}{Dt} = \frac{1}{\mathrm{Pr}}\nabla^2\theta + \lambda\theta, \tag{17}$$

where

$$\mathrm{Ra} = \frac{g\beta(\Delta T)^2 L^3}{\alpha\nu}, \quad \mathrm{Pr} = \frac{\nu}{\alpha}, \quad \lambda = \frac{Q_0 L_R^2}{\rho\nu C_p} \tag{18}$$

are the Rayleigh number, Prandtl number and the heat absorption parameter, respectively. Finally the boundary conditions are:

$$\begin{aligned} &U = 0, \quad V = 0, \quad \theta = \frac{T_H - T_0}{\Delta T} \quad \text{at } X = 0 \\ &U = 0, \quad V = 0, \quad \theta = \frac{T_C - T_0}{\Delta T} \quad \text{at } X = L \\ &U = 0, \quad V = 0, \quad \frac{\partial\theta}{\partial Y} = 0 \quad \text{at } Y = 0, H. \end{aligned} \tag{19}$$

In Eq. 1 the heat generation term is active only when $\theta > 0$.

Once the solutions of Eqs. 14, 15, 16 and 17 are known one may calculate the rate of heat transfer in terms of the Nusselt number at the left and right walls of the cavity using the following relation:

$$\mathrm{Nu} = -\left(\frac{\partial T}{\partial X}\right)_{X=0,H}. \tag{20}$$

An upwind finite-difference method together with the successive over-relaxation (SOR) iteration technique has been employed to solve Eqs. 14, 15, 16 and 17 which govern the flow. Details of this method have already been discussed in Hossain and Wilson [14] and are omitted for the sake of brevity. It is clear that the non-dimensional parameters of interest are the Rayleigh number, Ra, the Prandtl number, Pr, and the heat generation number, λ. In the present investigation, the value of the Prandtl number is chosen as 11.58, which corresponds to cold water, and that of the Rayleigh number as 10^5 for values of $\lambda = 0.0$, 1.0, 2.0, and 3.0. This value of the Rayleigh number is sufficiently large that convection is strong, but not sufficiently large that the flow becomes unsteady. Throughout the present investigation value of T_C has been set at 0°C.

The results shown and discussed in the following section have been calculated from zero initial velocities and mean values of temperature. A grid dependence study has been carried out for a thermally-driven cavity flow for the values of parameters $Ra = 10^5$, $Pr = 11.58$, $T_H = 8$°C, and $\lambda = 1.0$ with meshes of 43×43, 53×53 and 63×63 points and the resulting flow quantities are listed in Table 1.

Finally, to gain the confidence in the present algorithm, simulation of the natural convection is first performed without effect of internal heat source for values of $T_H = 3.98$, 8.0 and 12.0 while $Ra = 10^4$ and compared the results with that obtained by Tong and Koster [15] in terms of ψ_{max} and ψ_{min} (see Table 2) as well as the streamlines and the isotherms (Fig. 2) and these were found to be in excellent agreement.

For computational economy, a 43×43 mesh has been used throughout for the simulations described below. Finally, simulations were carried out until the steady state was obtained. For all sets of parameters considered it was found that the largest time, t, required to reach the steady state solution was roughly ten when using the time step $\Delta t = 10^{-4}$.

Table 1 Maximum and minimum values of ψ and θ for different sets of grids

$m \times n$	ψ_{min}	ψ_{max}	θ_{min}	θ_{max}
63×63	−6.724	3.810	−0.4904	0.5527
53×53	−6.797	3.760	−0.4905	0.5495
43×43	−6.907	3.699	−0.4905	0.5450

Table 2 Maximum and minimum values of ψ and θ for different T_h with 43×43 in square cavity while $Ra = 10^4$

T_H	Tong and Koster [9]		Present	
	ψ_{min}	ψ_{max}	ψ_{min}	ψ_{max}
3.98	0.0	15.318	0.0	15.706
8.00	−3.749	3.451	−3.800	3.461
12.00	−9.527	0.107	−9.740	0.114

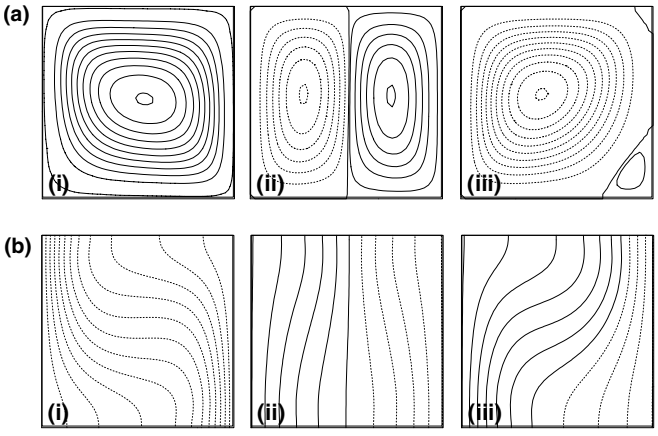

Fig. 2 Evaluation of **a** convective flow pattern and the **b** temperature field for different T_H: (i) 3.98, (ii) 8.0 and (iii) 12.0 while $Ra = 10^4$ and $\lambda = 0$. (These results are obtained by simulating the equations simulated by Tong and Koster [9])

3 Results and discussion

Some representative results are shown in Figs. 3, 4, 5, 6, 7, 8, 9 and 10 for $Ra = 10^5$ and $Pr = 11.58$. These figures show the effects of variation in the values of the heat generation parameter λ for three different aspect ratios, and for different values of T_H for a square cavity.

Figures 3 and 4 summarize how variations in the value of λ affect the flow and temperature fields for a square cavity with $T_H = 8$. When there is no heat generation and the sidewall temperatures are equally far from T_0, which corresponds to the maximum density, it is natural that the streamlines and isotherms display certain symmetries about the central vertical line. Each sidewall generates an identical upward buoyancy force, and therefore a two-cell flow is obtained with fluid flowing down the middle of the cavity. Indeed any variation in the values of T_H and T_C away from cases where $T_0 = (T_H + T_C)/2$ will cause the flow to become asymmetric due to different buoyancy forces on the sidewalls. Figure 3a(i) shows a situation, which is very close to symmetry since T_H-T_0 is almost the same as T_0-T_C. As $T_0 = 3.98$°C is slightly less than the mean temperature of the sidewalls, which is 4°C, the buoyancy force exerted at the hot wall is slightly greater than that at the cold wall. Therefore there is a slightly stronger clockwise circulation than anticlockwise.

This asymmetric effect may be seen increasingly in frames (ii–iv) of Fig. 3 where nonzero values of λ are used. The heat generation principle of Vajravelu and Hadjinicolaou [19] is such that heat is generated only when $T > T_0$ ($\theta > 0$), and this serves to destroy the near-symmetry found in Fig. 3a. There is now a stronger buoyancy force on the left-hand hot wall because of heat generation than on the cold wall, and therefore the hot stream is able to push further across the top of the square. Although the flow becomes stronger, the thermal boundary layer becomes thicker, which causes a reduc-

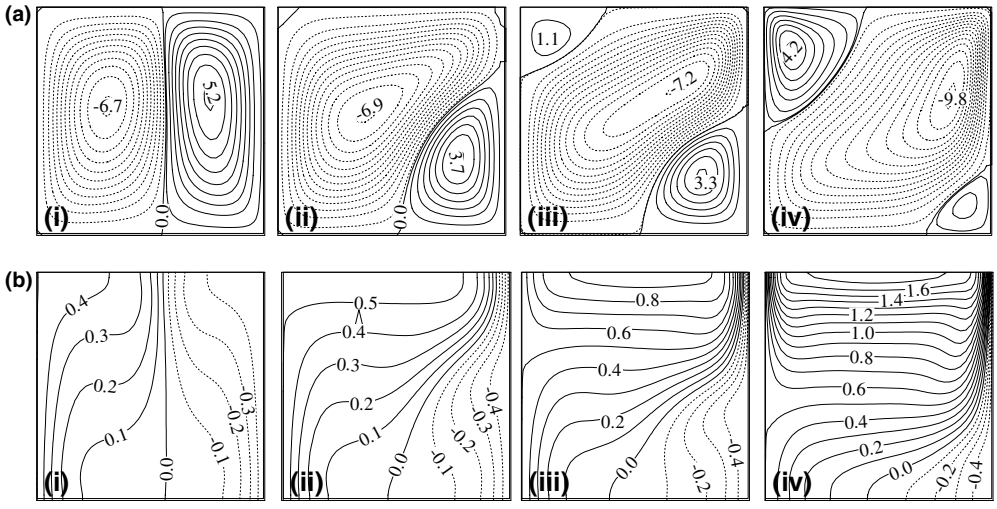

Fig. 3 **a** Streamlines at steady state for different λ: (i) 0.0, (ii) 1.0, (iii) 2.0 and (iv) 3.0 with dimension $D = 1{:}1$ while $\mathrm{Ra} = 10^5$, $\mathrm{Pr} = 11.58$ and $T_H = 8°C$. **b** Isotherms at steady state for different λ: (i) 0.0, (ii) 1.0, (iii) 2.0 and (iv) 3.0 with dimension $D = 1{:}1$ while $\mathrm{Ra} = 10^5$, $\mathrm{Pr} = 11.58$ and $T_H = 8°C$

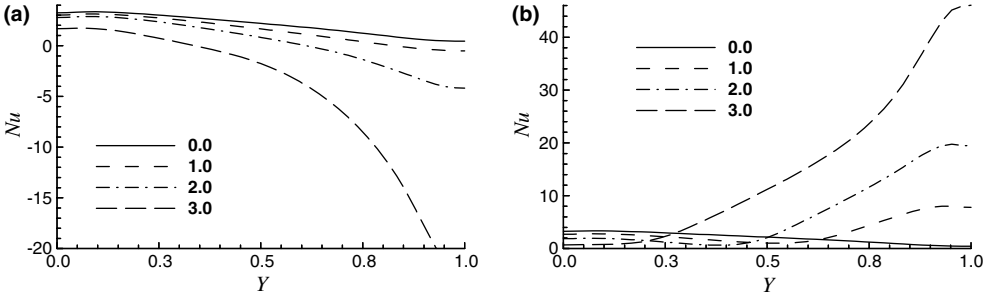

Fig. 4 Steady state Nusselt number at **a** left wall **b** right wall for different λ: (i) 0.0, (ii) 1.0, (iii) 2.0 and (iv) 3.0 with dimension $D = 1{:}1$ while $\mathrm{Ra} = 10^5$, $\mathrm{Pr} = 11.58$ and $T_H = 8°C$

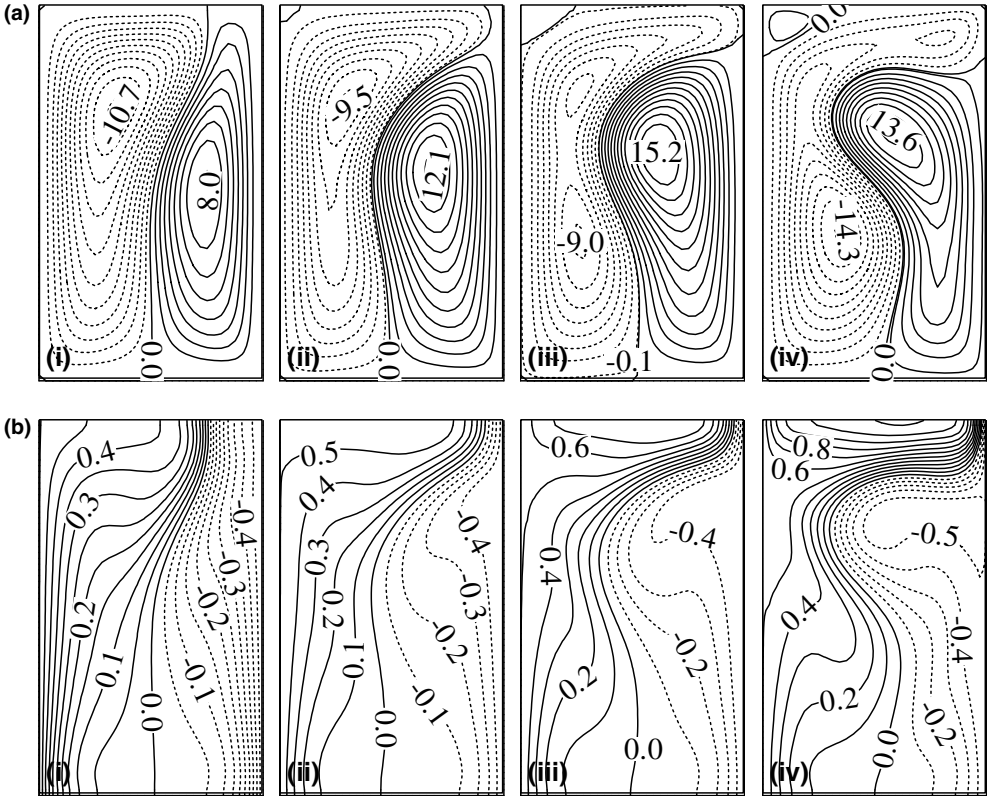

Fig. 5 Streamlines at steady state for different λ: (i) 0.0, (ii) 1.0, (iii) 2.0 and (iv) 3.0 with dimension $D = 1{:}2$ while $\mathrm{Ra} = 10^5$, $\mathrm{Pr} = 11.58$ and $T_H = 8°C$. **b** Isotherms at steady state for different λ: (i) 0.0, (ii) 1.0, (iii) 2.0 and (iv) 3.0 with dimension $D = 1{:}2$ while $\mathrm{Ra} = 10^5$, $\mathrm{Pr} = 11.58$ and $T_H = 8°C$

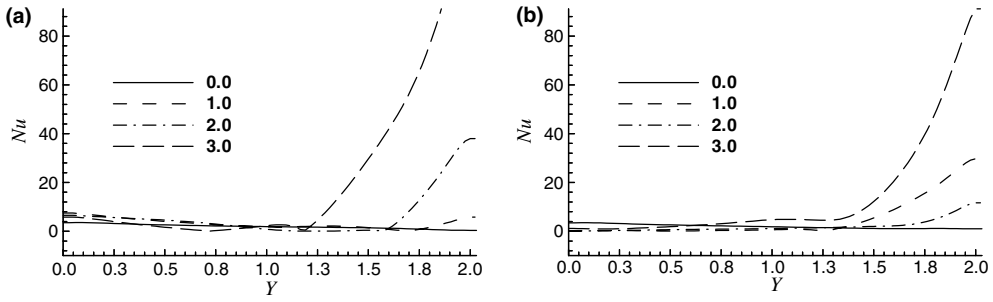

Fig. 6 Steady state Nusselt number at **a** left wall and **b** right wall for different λ: (i) 0.0, (ii) 1.0, (iii) 2.0 and (iv) 3.0 with dimension $D = 1{:}2$ while $\mathrm{Ra} = 10^5$, $\mathrm{Pr} = 11.58$ and $T_H = 8°C$

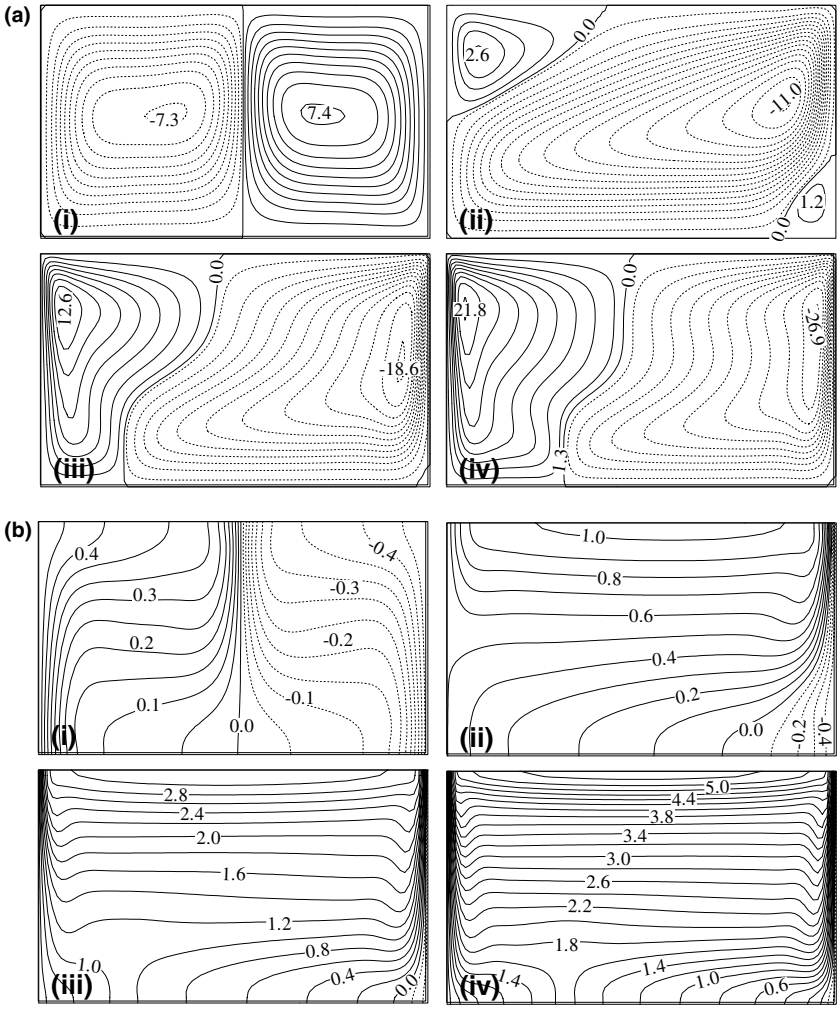

Fig. 7 Streamlines at steady state for different λ: (i) 0.0, (ii) 1.0, (iii) 2.0 and (iv) 3.0 with dimension $D = 2{:}1$ while $\mathrm{Ra} = 10^5$, $\mathrm{Pr} = 11.58$ and $T_H = 8°C$. **b** Isotherms at steady state for different λ: (i) 0.0, (ii) 1.0, (iii) 2.0 and (iv) 3.0 with dimension $D = 2{:}1$ while $\mathrm{Ra} = 10^5$, $\mathrm{Pr} = 11.58$ and $T_H = 8°C$

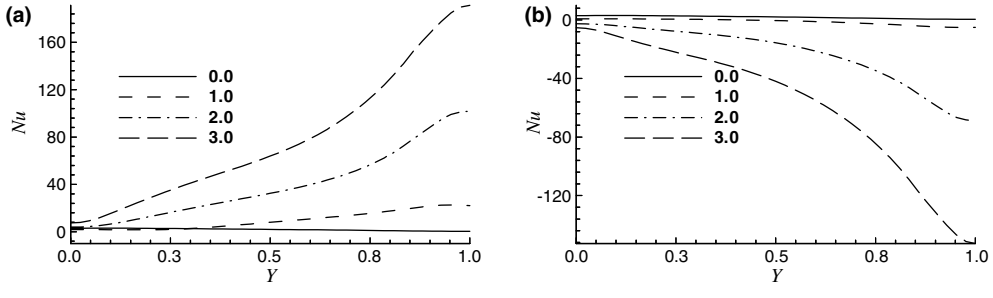

Fig. 8 Steady state Nusselt number at **a** left wall and **b** right wall for different λ: (i) 0.0, (ii) 1.0, (iii) 2.0 and (iv) 3.0 with dimension $D = 2{:}1$ while $\mathrm{Ra} = 10^5$, $\mathrm{Pr} = 11.58$ and $T_H = 8°C$

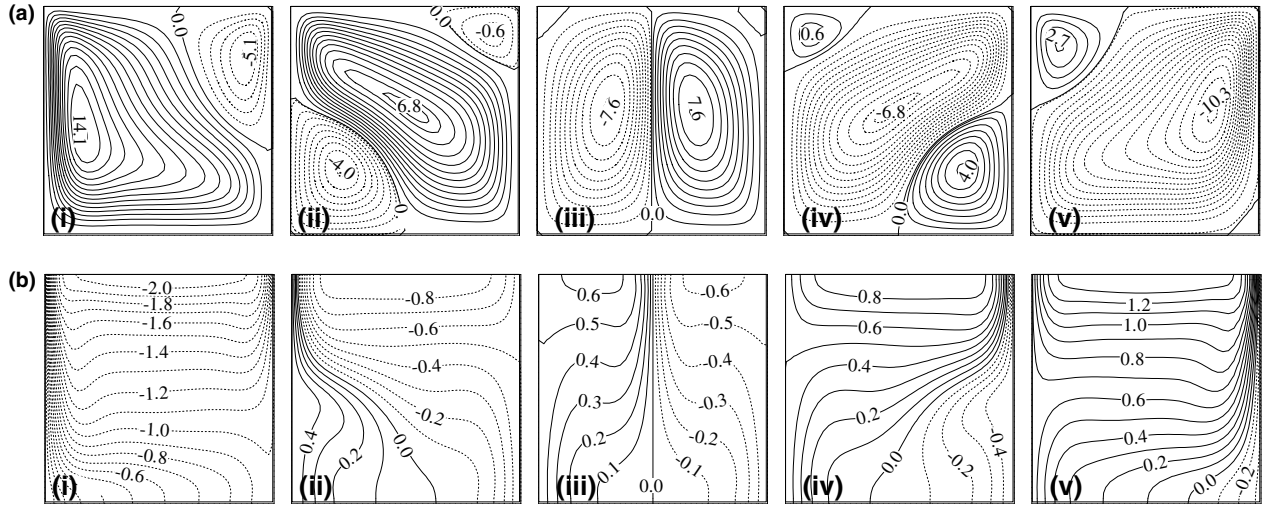

Fig. 9 Streamlines at steady state for different T_H: (i) 4°C, (ii) 7.95°C, (iii) 7.96°C, (iv) 7.97°C and (v) 12.0°C with dimension $D = 1{:}1$ while $Ra = 10^5$, $Pr = 11.58$ and $\lambda = 2.0$. **b** Isotherms at steady state for different T_H: (i) 4.0°C, (ii) 7.95°C, (iii) 7.96°C, (iv) 7.97°C and (v) 12.0°C with dimension $D = 1{:}1$ while $Ra = 10^5$, $Pr = 11.58$ and $\lambda = 2.0$

tion in the rate of heat transfer on the left-hand wall. Conversely, the fact that the hot jet impinges on the cold, right hand surface means that the rate of heat transfer on the cold wall increases near the top right hand corner.

However, when λ is as large as 2, the heat generation effect is sufficiently strong to raise the internal fluid temperature higher than that of the hot sidewall. This causes a change in sign of the heat transfer (see Fig. 4a), and therefore the hot surface is cold relative to the fluid in the top left hand corner. Thus the possibility of thermal runaway is avoided by having heat lost through the upper part of both sidewalls. The presence of hot fluid close to a relatively cold wall means that buoyancy forces now act downwards in the top left hand corner of the cavity, and therefore we see a recirculation region becoming stronger as λ increases.

Figures 5 and 6 display the corresponding situation for a tall cavity of aspect ratio 2. The same trends occur here, namely that we have a nearly symmetric flow and isotherm pattern in the absence of heat generation, and the progressive protrusion of the hot boundary layer across the top of the cavity, as λ increases, and into the region near the cold sidewall. The main phenomenological difference is that the increased strength of the upward boundary layers compared with those in the square cavity, causes the cold boundary layer to be ejected from the wall and into the bulk of the flow. Thus the recirculating region in the bottom two thirds of the cold half develops a bulge as the boundary layer separates while still travelling slightly upwards. The increased height of the cavity yields a greater vertical distance over which buoyancy forces can accelerate the fluid, and therefore the magnitude of the surface rates of heat transfer are considerably greater for this cavity than for the square cavity.

We now turn to a shallow cavity of aspect ratio 2, as shown in Figs. 7 and 8. Near-symmetry persists once more when $\lambda = 0$. However, the greater width of the cavity means that a much larger expanse of fluid is at temperatures greater than $\theta = 0$, and much of this is situated far from the sidewalls. Therefore there is potential for the fluid temperature to rise considerably relative to the earlier two cases which correspond to narrower cavities. Thus we see that heat generation is sufficient powerful that the top left recirculation grows so much in strength when λ is as large as three, that it forms a very strong downward boundary layer on the hot surface. Therefore we have what is an extremely strange situation, namely that the agency of heat generation has transformed a flow consisting of ascending boundary layers up the sidewalls (see Fig. 7a) into one where there are descending boundary layers on the sidewalls. The above comments regarding the increasing potential for large temperatures is borne out in Fig. 8 where the local Nusselt numbers for

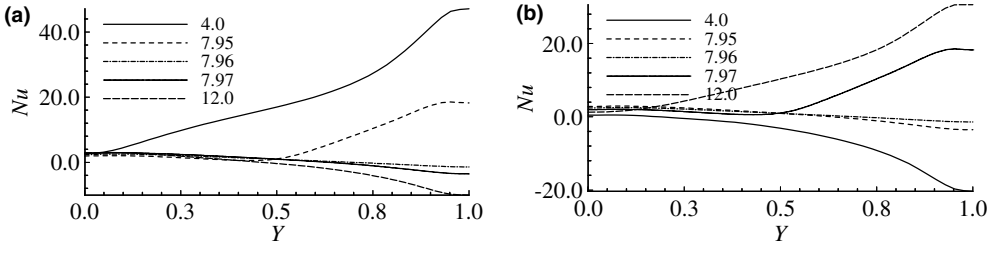

Fig. 10 Steady state Nusselt number at **a** left wall and **b** right wall for different T_H: (i) 4.0°C, (ii) 7.95°C, (iii) 7.96°C, (iv) 7.97°C and (v) 12.0°C with dimension $D = 1{:}1$ while $Ra = 10^5$, $Pr = 11.58$ and $\lambda = 2.0$

$\lambda \neq 0$ are considerably bigger than those for the square cavity.

Finally we see in Figs. 9 and 10 the effect of increasing T_H in a square cavity with all other parameters held fixed, and with $\lambda = 2$. The reference case is shown in Fig. 9a(i), b(i). An increase in T_H means that we have an increase in the heat generation effect. Associated with that is the increasing size of the top left recirculation region, as discussed earlier, and the corresponding rise in the temperature in the upper half of the cavity is seen clearly in Fig. 8b. When T_H is relatively small [see Figs. 3a (iv), b (iv) and 9a (iv), b (iv)], there remains an ascending boundary layer in the bottom right hand corner of the cavity, since buoyancy forces are positive. However, the increasing strength of the left-hand upward flow progressively kills this ascending boundary layer as T_H increases. Therefore we see the bottom right recirculation region decreasing in size as λ increases. Increased rates of heat transfer accompany increases in T_H quite naturally.

4 Conclusions

In this paper we have investigated convective flow in a cavity which is induced by differential heating of the sidewalls and assisted by internal heating. Attention has been focused on convection near the density minimum for water and the Prandtl and Rayleigh numbers have been fixed at $Pr = 11.58$ and $Ra = 10^5$. It has been found that the flow and temperature field depend very strongly on the internal heat generation parameter, λ, and the difference between T_0 and the mean temperature of the sidewalls. When the mean temperature is the same as T_0 then the flow is symmetric, but the symmetry is broken when either the mean temperature or λ varies. It has also been found that when λ is sufficiently strong, the circulation of the flow is reversed.

References

1. Han SM (1984) A transient numerical analysis of high Rayleigh number convection in a different end heated square cavity. ASME paper 84:HT-57
2. Ivey GN (1984) Experiments on transient natural convection in a cavity. J Fluid Mech 144:443–447
3. Nicolette VF, Yang KT, Lloyd JR (1985) Transient cooling by natural convection in a two dimensional square enclosure. Int J Heat Mass Transfer 28:1725–1732
4. Hall JD, Bijan A, Chaddock JB (1988) Transient natural convection in a rectangular enclosure with one heated side wall. Int J Heat Fluid Flow 9:396–404
5. Watson A (1972) The effect of inversion temperature on the convection of water in an enclosed rectangular cavity. Q J Mech Appl Math 25:423–446
6. Lin DS, Nansteel MW (1987) Natural convection heat transfer in a square enclosure containing water near its density maximum. Int J Heat Mass Transfer 30:2319–2329
7. Seki N, Fukusako S, Inaba H (1978) Free convective heat transfer with density inversion in as confined rectangular vessel. Heat Mass Transfer 11:145–156
8. Desai VS, Forbes RE (1971) Free convection in water in the vicinity of maximum density. Eng Geophys Heat Transfer 4:41–47
9. Tong W, Koster JN (1993) Coupling of natural convection flow across a vertical density inversion interface. Warme- Und Stoffbertragung 28:471–479
10. Forbes RE, Cooper JW (1975) Natural convection in a horizontal layer of water cooled from above to near freezing. ASME J Heat Transfer 97:47–53
11. Vasseur P, Robillard L (1980) Transient natural convection heat transfer in a mass of water cooled through 4°C. Int J Heat Mass Transfer 23:1195–1205
12. Robillard L, Vasseur P (1981) Transient natural convection heat transfer of water with maximum density and super cooling. ASME J Heat Transfer 103:528–531
13. Robillard L, Vasseur P (1982) Convective response of a mass of water neat 4 °C to a constant cooling rate applied to its boundaries. J Fluid Mech 118:123–141
14. Oosthuizen PH, Paul JT (1990) Unsteady free convective flow in an enclosure containing water near its density maximum. HTD 140:83–91
15. Tong W, Koster JN (1993) Natural convection of water in a rectangular cavity including density inversion. Int J Heat Fluid Flow 14:366–375
16. Debler WR (1966) On the analogy between thermal instability and rotational hydrodynamic stability. J Fluid Mech 24:165–176
17. Sun Z-S, Tien C, Yen Y-C (1969) Thermal instability of a horizontal layer of fluid with maximum density. A I Ch E Jl 15:910–915
18. Gebhart B, Mollendorf JC (1977) A new density relation for pure and saline water. Deep Sea Res 24:831–848
19. Vajravelu K, Hadjinicolaou A (1997) Convective heat transfer in an electrically fluid at a stretching surface with uniform free stream. Int J Eng Sci 34:1237–1244
20. Hossain MA, Wilson M (2002) Natural convection flow in a fluid-saturated porous medium enclosed by non-isothermal walls with heat generation. Int J Thermal Sci 41:447–454